JOURNAL OF GEOPHYSICAL RESEARCH, VOL. 106, NO. E3, PAGES 5033–5041, MARCH 25, 2001

Acoustic environment of the Martian surface

Jean-Pierre Williams

Department of Earth and Space Sciences, University of California, Los Angeles

Abstract. Prompted by the Mars Microphone aboard the 1998 Mars Polar Lander, a theoretical study of the acoustical environment of the Martian surface has been made to ascertain how the propagation of sound is attenuated under such conditions and to predict what sounds may be detectable by a microphone. Viscous and thermal relaxation (termed classical absorption), molecular relaxation, and geometric attenuation are considered. Classical absorption is stronger under Martian conditions resulting in sounds in the audible frequencies (20 Hz to 20 kHz) being more strongly attenuated than in the terrestrial environment. The higher frequencies (>3000 Hz) will be severely attenuated as the absorption is frequency dependent. At very low infrasound frequencies (i.e., < 10 Hz), attenuation will be mostly due to geometric spreading of the propagating wave front and will therefore be more similar to the terrestrial surface environment. Probable sound sources in the landed environment include wind-blown dust and sand from large dust storms, dust devils, and possible associated electrostatic discharge. The sounds most likely to be detected will be sounds generated by the lander itself and aeroacoustic noises generated by winds blowing against the lander and its instruments.

1. Introduction

The 1998 Mars Polar Lander (MPL), which was to land in the south polar region of Mars (76°S, 195°W) on December 3, 1999, had on board a microphone that would have offered the unique opportunity to sample the acoustic environment on the surface of Mars. The Mars Microphone, which was funded by The Planetary Society as part of the LIDAR experiment, was to provide a 2.5 s sound sample in the 20 kHz sampling mode or a 10.6 s sound sample in the 5 kHz sampling mode every week (G. T. Delory et al., unpublished manuscript, 2000). A theoretical study has been undertaken to characterize the acoustic environment at the surface of Mars to estimate what a microphone in such an environment might be expected to detect and qualify the conditions for future acoustic instrumentation.

The atmospheric environment at the landing site is similar to the Earth's stratosphere in terms of temperature and pressure. The atmospheric pressure will be ~6–8 mbars, and the temperatures are expected to be around 200–240 K. A microphone in this environment is expected to detect sounds within close proximity, although the sounds will be attenuated relative to the terrestrial surface environment.

In characterizing the atmospheric acoustics of Mars, the atmosphere can be treated as a continuous compressible media in which oscillatory motion occurs. Deformations are transmitted as pressure fluctuations in all directions from the point where they arise. These pressure waves and their propagation through the atmosphere have been modeled to better understand the sound speed, intensity, attenuation, and detectability by an acoustic sensor.

Paper number 1999JE001174.
0048-0227/01/1999JE001174$9.00

2. Speed of Sound on Mars

The speed of sound in the Martian atmosphere can be derived by assuming the atmosphere to be an elastic continuum in which there is no rigidity. Such a medium will transmit only longitudinal waves. The compressions and rarefactions of the propagating waves occur fast enough that they can be treated adiabatically. The relation PV^{γ} = constant is employed, where γ is the ratio of the specific heat of the gas at constant pressure to the specific heat of the gas at constant volume, and therefore depends on the properties of the gas. For a CO_2 atmosphere at 220 K, $\gamma \approx 1.338$. With the use of the ideal gas law, the sound speed, c, can be expressed as

$$c \approx \sqrt{\gamma \frac{R^* T}{M}}, \tag{1}$$

where R^* is the universal gas constant (8.314 j mol^{-1} K^{-1}) and M is the mean molecular weight of the air. Thus the speed of sound depends only on the temperature and composition of the gas.

The region of the MPL landing site is blanketed by seasonal frost cover during the southern winter and early spring, which sublimates away with the onset of summer. The Lander was to arrive in late spring at Ls = 256, where Ls is the areocentric longitude of the Sun. The frost cover should have sublimated from the landing site several weeks before arrival. Small patches of frost may still have remained in low-lying topography where it remained shielded from receiving prolonged direct sunlight. Given that the 6 mbar frost point of CO2 is ~147 K, early in the mission, local surface temperatures may have been very cold, but Viking Infrared Thermal Mapper (IRTM) data from the 20-μm channel indicates average surface temperatures between 205 to 240 K at this season (M. Richardson, personal communication, 1999). This range of temperatures gives a sound speed ranging from 227 to 246 m/s. For comparison

the sound speed on Earth is 343 m/s at room temperature (T=293 K) and 1 bar of pressure.

3. Wave Energy and Intensity

3.1. Particle Displacement and Velocity

The propagation of sound through the atmosphere occurs by means of wave motion and therefore can be described by the wave equation, which for a plane wave of a particular wavenumber, k, and angular frequency, ω, traveling in the positive x direction has the following solution:

$$p(x,t) = p_o \exp[i(kx - \omega t)], \tag{2}$$

where p_o is the amplitude.

With the excess pressure p_o of the sound wave, there is a displacement of the medium from equilibrium. Assuming that the particle displacement is small, the strain tensor for hydrostatic compression can be expressed as (see *Mase* [1970] for details)

$$\varepsilon_{ii} = \frac{\partial u_i}{\partial x_i} = -\frac{p}{K}, \tag{3}$$

where K is the bulk modulus (or the modulus of hydrostatic compression) and $K = \rho_o c^2$. Substituting (2) into (3) and integrating gives the particle displacement
and the particle velocity

$$u = \frac{p_o}{2\pi f \rho_o c} \sin(kx - \omega t), \tag{4}$$

$$v = \frac{du}{dt} = -\frac{p_o}{\rho_o c} \cos(kx - \omega t). \tag{5}$$

3.2. Sound Intensity

The energy transported by the acoustic waves through the continuum is in two forms: kinetic energy from the particle motion and potential energy from the compressed elastic medium. When the particle moves through the equilibrium position, the kinetic energy is at a maximum, and the potential energy is zero. Since the total energy is conserved and in an adiabatic fluid, it may be measured as the maximum kinetic energy. The kinetic energy is

$$E_k = \frac{1}{2}\rho_o V_o v^2 = \frac{1}{2}\frac{p_o^2 V_o}{\rho_o c^2} \cos^2(kx - \omega t), \tag{6}$$

where V_o is volume and the total energy density is

$$U = \frac{1}{2}\frac{p_o^2}{\rho_o c^2}. \tag{7}$$

The intensity of a sound wave is the time average rate of flow of energy through unit area of the medium perpendicular to the direction of propagation. Put another way, it is the energy density flux, which is the product of the energy density and the sound speed.

$$I = Uc = \frac{1}{2}\frac{p_o^2}{\rho_o c} \tag{8}$$

The intensity level of sounds is often measured in decibels (dB), which is based on a logarithmic scale. One reason for doing this is because of the wide range of pressures and intensities encountered in the acoustic environment. Audible intensities range from 10^{-12} to 10 W m^{-2} [*Kinsler et al.*, 1982]. Another reason for doing this is that humans judge the relative loudness of two sounds by the ratio of their intensities, i.e., logarithmically. Using a fixed reference level of sound intensity I_o (10^{-12} W m^{-2}), the sound level in decibels becomes

$$\beta = 10\log_{10}\frac{I}{I_o}. \tag{9}$$

4. Attenuation of Sound Waves

4.1. Classical and molecular absorption

As the sound wave propagates through the atmosphere, it will experience a loss in internal energy. This dissipation of acoustic energy results in the decline in the intensity as a function of distance from the source. This can be attributed to viscosity of the CO_2 gas and thermal conduction, collectively termed classical absorption, and molecular relaxation.

Viscosity, thermal conduction, and molecular relaxation dissipate the acoustic energy as heat. This diminishes the amplitude over time in a way that is analogous to a damped wave in a string [see *Marion and Thorton*, 1995]. In this situation, (2) becomes

$$p = p_o \exp(-\alpha x)\exp[i(kx - \omega t)], \tag{10}$$

where α is the absorption coefficient and acts to dampen the wave as it propagates. Each loss mechanism has an associated absorption coefficient, which contributes to damping the acoustic wave (Figures 1 and 2).

The viscosity of the atmosphere arises from friction within the fluid, which produces a delay between the application of the pressure change and attainment of the corresponding equilibrium density. This effect is accounted for by introducing a relaxation time τ into the equation of state [see *Kinsler et al.*, 1982] where, assuming the relaxation time to be short, the absorption coefficient can be expressed as

$$\alpha_v = \frac{1}{2}\frac{\omega^2 \tau}{c}. \tag{11}$$

To determine the relaxation time, the Navier-Stokes equation of motion for an irrotional, compressible fluid is employed, and τ can be identified as

$$\tau = \frac{4}{3}\frac{\eta}{\rho_o c^2}, \tag{12}$$

where η is the viscosity coefficient. From this, the absorption coefficient for viscosity becomes

$$\alpha_v = \frac{2}{3}\frac{\omega^2 \eta}{\rho_o c^3} = \frac{8}{3}\frac{\pi^2 f^2}{\rho_o c^3}\eta. \tag{13}$$

As can be seen from this equation for the absorption coefficient, attenuation is proportional to the square of the frequency, f, and therefore the higher frequencies will be more strongly attenuated (Figure 1). The coefficient is also inversely proportional to the cube of the sound speed. Since the sound speed is lower on Mars than on Earth, the attenuation due to viscosity is also more effective. For Mars,

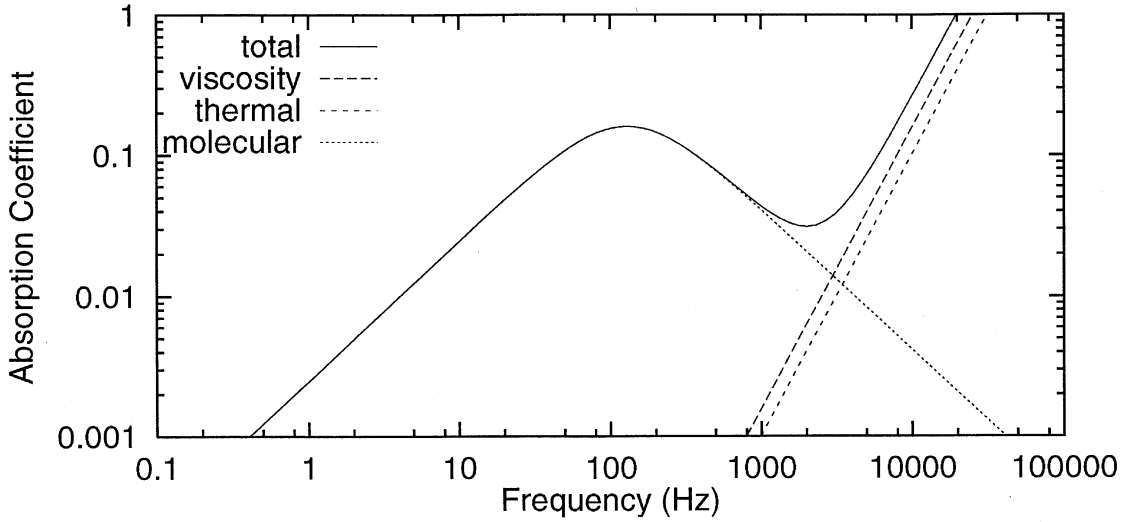

Figure 1. Absorption coefficients as a function of frequency for a 6 mbar CO_2 atmosphere at 220 K. Long-dashed lines represent absorption due to viscosity, medium-dashed lines represent absorption from thermal diffusion, and short-dashed lines represent absorption from molecular relaxation. Viscosity coefficient η=11.19x10^{-6} N s m^{-2} used from *Touloukian et al.* [1975]. Values for thermal conductivity (0.01083 W m^{-1} K^{-1}) and heat capacity (568.1 J kg^{-1} K^{-1}) from *Touloukian et al.* [1970] and *Keenan et al.* [1983], respectively. Value of 0.16 for μ_{max} and 129 Hz for f_M is extrapolated from *Shields* [1957].

α_v is (1.568x10^{-9})f^2, for a temperature of 220 K where on Earth at room temperature α_v is (8.31x10^{-11})f^2.

The loss of energy due to thermal conduction occurs because the pressure fluctuations associated with the sound wave are not in thermodynamic equilibrium. Although the sound propagation has been treated as occurring adiabatically up to this point, in actuality heat will flow irreversibly in the presence of a temperature gradient [*Morse and Ingard,* 1968].

The compression and rarefaction of the passing wave will create warmer and cooler regions which will cause a diffusion of heat energy. The flux of heat is proportional to the negative gradient of the temperature where the constant of proportionality is the thermal conductivity K. The change in internal energy can be expressed as the negative divergence of the flux. Using this with the second law of thermodynamics, a relation for the rate of change of entropy for a unit mass per unit volume can be established [see *Morse and Ingard*, 1968]. Energy will be withdrawn with each unit distance traveled and the absorption coefficient associated with thermal conductivity will be

$$\alpha_T = \frac{dQ}{I} = \left(\frac{\gamma - 1}{\gamma}\right)\frac{4\pi^2 f^2 K}{\rho_o c^3 C_V}, \tag{14}$$

where C_V is the heat capacity at constant volume.

Like the absorption coefficient for viscosity, absorption due to thermal diffusion is a function of the frequency squared. The higher frequencies are damped out faster as heat energy is diffused more effectively at higher frequencies

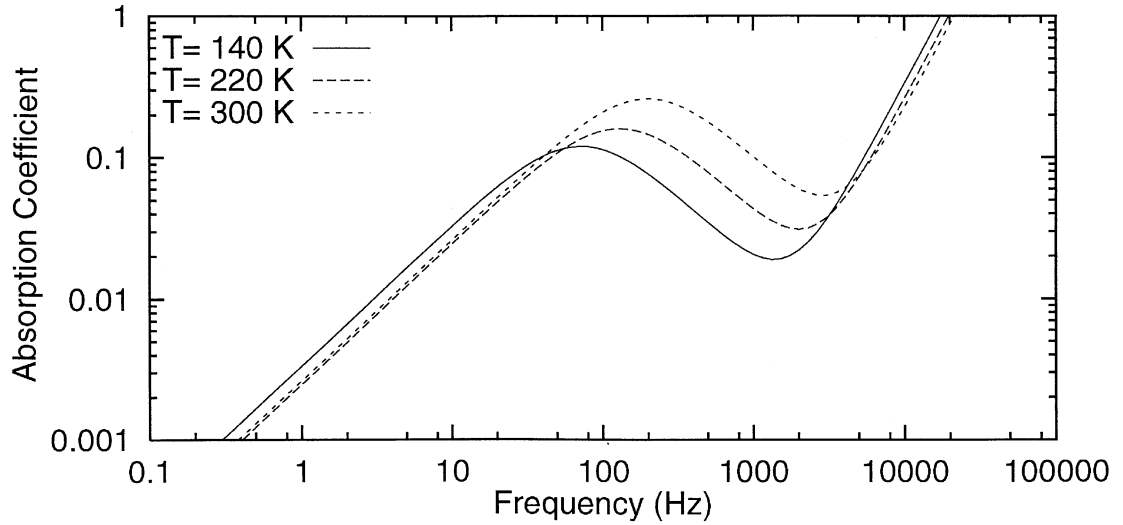

Figure 2. Total absorption coefficient for two temperature extremes, 140 K (solid line), 300 K (short-dashed line), and the nominal case, 220 K (long-dashed line).

(Figure 1). The colder Martian environment leads to a larger absorption coefficient, $(1.01\text{x}10^{-9})f^2$ for Mars at a temperature of 220 K and $(7.90\text{x}10^{-11})f^2$ for the Earth atmosphere at room temperature.

The classical absorption mechanisms do not account for all of the observed attenuation of sound in diatomic and polyatomic gases. One must take into account that in addition to the translational degrees of freedom of the molecule, there are internal degrees of freedom associated with rotation and vibration. When the gas is locally compressed in the passage of the sound wave, the average translational kinetic energy increases. Some of this translational energy goes into rotational and vibrational energy. This occurs more slowly than the near instantaneous change in translational energy and is associated with a relaxation time.

The amount of energy lost from this is related to the ratio between the length of the cycle and the relaxation time. If the compression and rarefaction of the passing wave is fast compared to the relaxation time, little energy will have had time to transfer into the rotation and vibration of the molecules, and the gas will act as a monatomic gas. Likewise, if the length of the cycle is much longer than the relaxation time, the gas will be able to maintain a constant state of thermal equilibrium and there will be no attenuation from relaxation. This effect will therefore be important for an intermediate range of frequencies (for further discussion, see *Kinsler et al.* [1982]).

The specific heat at constant volume is the rate of change of the internal energy of the gas with temperature at constant volume. As a result of molecular relaxation, the specific heat will have a frequency dependence and an associated relaxation time. Substituting this into the wave equation yields the expression for the attenuation coefficient

$$\alpha_f = \frac{2\mu_{\max} f_M f}{f_M^2 + f^2}, \tag{15}$$

where $\mu_{\max}$ is the maximum value of the function plotted against the log of the frequency and f_M is the corresponding frequency.

An experimental study of the thermal relaxation in carbon dioxide has been carried out by *Shields* [1957] for temperatures between 0° and 200°C at 1 atm of pressure. The value of $\mu_{\max}$ was extrapolated from the trend in these results for Martian surface temperatures resulting in a $\mu_{\max}$ of ~0.16 corresponding to a temperature of 220 K. Decreasing the pressure has the same effect on absorption as increasing the frequency and hence f_M is attained by shifting the plot of $\mu_{\max}$ against frequency per pressure accordingly. This results in the strongest attenuation occurring around 129 Hz (see Figure 1).

The effects of all three energy loss mechanisms can be combined by summing the absorption coefficients together as if they were calculated separately which does not introduce errors for the frequency range being dealt with here [*Kinsler et al.*, 1982]. The results of this are shown in Figure 1, which shows the absorption coefficient as the sum of the three coefficients as a function of frequency. As diurnal and seasonal temperatures can fluctuate considerably, the absorption coefficient has been calculated for two separate temperature extremes, 140 K and 300 K (Figure 2). Figure 3 shows the effects of these absorption mechanisms on the sound intensity at three distances from the sound source, 10, 100, and 1000 m (T=220 K). As can be seen, the high frequencies damp out relatively quickly and only the lowest frequencies travel large distances.

From Figures 1-3 it can be seen that at frequencies greater than 3 kHz, classical absorption is the dominant mechanism for attenuation. At frequencies below 1 kHz molecular absorption begins to dominate attenuation. Between these two regimes, a "window" exists in which attenuation is reduced and sound can more readily propagate greater distances (Figure 3).

4.2. Geometrical Attenuation – Spherical Waves

When a sound is emitted by a source, the wave propagates away equally in all directions. At a close proximity the wave front will therefore be spherical in nature. The average rate of energy flow through a spherical surface of radius r is

$$W = 4\pi r^2 I, \tag{16}$$

which means that as the wave front grows as r^2, the intensity will decline as r^{-2}. For distances much larger than a wavelength ($r \gg \lambda$), any finite portion of the sphere through which the sound wave passes will be more nearly planar, and the wave fronts can be described more accurately as plane waves.

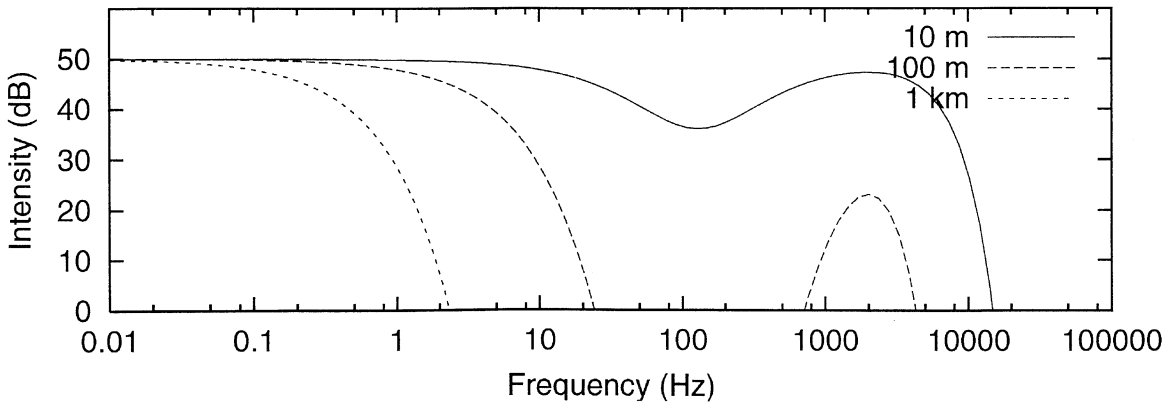

Figure 3. The intensity of a 50 dB sound source as a function of frequency at distances 10, 100, and 1000 m from the source. The "window" in the atmosphere between frequencies 1 and 3 kHz, where the region that molecular absorption dominates transitions into a region where classical absorption dominates, is evident.

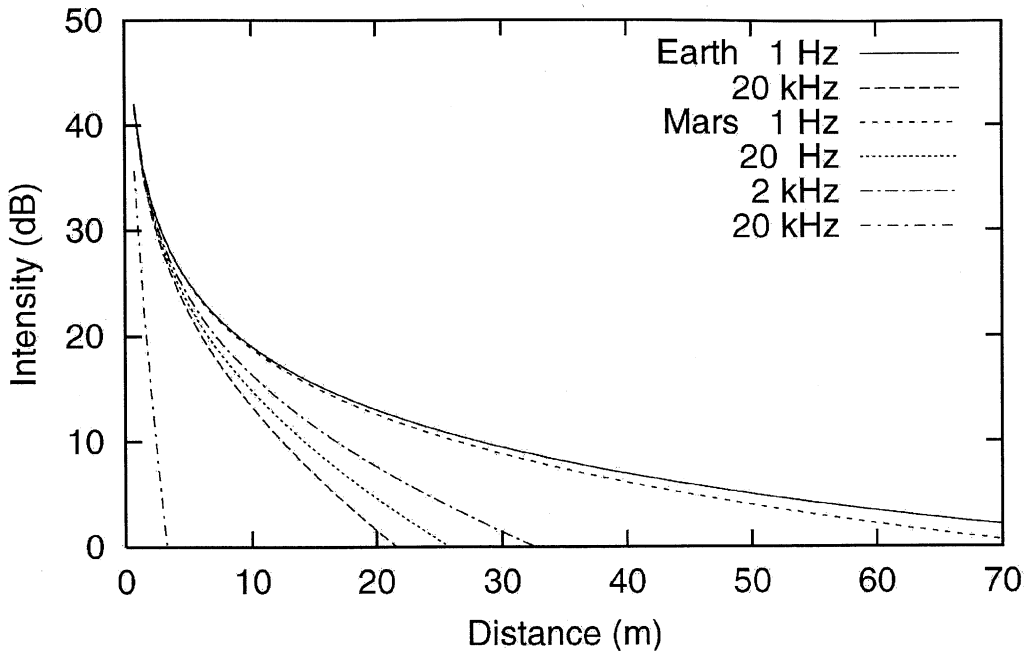

Figure 4. A 50 dB sound source at 1 Hz, 20 Hz, 2 kHz, and 20 kHz on Mars and 1 Hz and 20 kHz on Earth as a function of distance, taking into account a spherical wave front. It can be seen that attenuation is significantly greater on Mars compared to Earth assuming a standard terrestrial atmosphere of T=20°C, p=1bar, and relative humidity 37% (attenuation coefficient obtained from *Piercy* [1969]). The influence of molecular attenuation on the lower frequencies on Mars is evident as the 20 Hz signal is attenuated more then the 2 kHz signal. At very low frequencies, the classical and molecular attenuation become less effective and attenuation resembles that of the terrestrial environment as can be seen from the 1 Hz signal on Mars and Earth.

Figure 4 shows the intensity of a 50 dB source at frequencies 1 Hz, 20 Hz, 2 kHz, and 20 kHz on Mars and 1 Hz and 20 kHz on Earth as a function of distance from the source. As can be seen, the intensity will diminish rapidly relative to sound in the terrestrial atmosphere. The highest frequencies in the audible range will be severely attenuated, the 20 kHz signal only traveling a few meters. Molecular relaxation will cause an increase in attenuation in the lower frequencies of the audible frequency range. This is evident as the 20 Hz signal is attenuated to a greater extent then the 2 kHz signal.

Sounds in the infrasound frequency range below 10 Hz will be able to propagate larger distances as the classical and molecular absorption at these frequencies is small and geometric spreading of the wave front will be the dominant mechanism for sound attenuation. Therefore this range of the acoustic spectrum may be the most useful for detection of acoustic sources at an appreciable distance.

4.3. Propagation Near the Ground

For sound sources propagating almost horizontally near the ground, the acoustic properties of the ground become a major factor, specifically its acoustic impedance, the value of which can differ greatly with varying surfaces and increases with decreasing frequency [*Embleton*, 1996]. Treating the ground as a locally reacting porous surface, an amplitude reflecting coefficient, Rp can be defined [*Chessell*, 1977]

$$R_p = \frac{\sin\varphi - Z_1/Z_2}{\sin\varphi + Z_1/Z_2}, \qquad (17)$$

where φ is the grazing angle, Z_1 is the characteristic impedance of the air, equal to ρc, and Z_2 is the complex acoustic impedance, equal to $R+iX$, of the locally reacting surface (see *Morse and Ingard* [1968] and *Piercy et al.* [1977] for a detailed discussion). Multiplying (10) by Rp yields the resulting sound pressure of a ground-reflected ray.

Chessell [1977], expanding on the earlier work of *Delaney and Bazley* [1970], developed an empirical model of the acoustic impedance involving only one parameter, the specific flow resistance per unit thickness (σ). In some situations, *Attenborough* [1983] found better agreement with observations using five parameters, all relating to the ground material, the most significant being the specific flow resistance and porosity which can be combined into a single parameter described as an "effective flow resistivity" (σ_e). *Embleton et al.* [1983] list values of effective flow resistivity for various ground surfaces ranging in value from 10-30 kPa s^{-1} m^{-2} for freshly fallen snow to ~30000 kPa s^{-1} m^{-2} for mature asphalt.

The acoustic impedance of the landing site is difficult to predict as the surface properties of the layered terrain are completely unknown [*Vasavada et al.*, 2000]. If the surface is very hard, for example consisting of hard-packed, fine-grained dust (σ_e = 5000 – 20,000), then it will have a small effect. If a thick mantling of soft dust or frost or an accumulation of sand size particles is present (σ_e = 10 – 800), then the influence of acoustic impedance will be larger. At a frequency of 100 Hz, this gives a possible range of R_p values of 0.548-0.998 for a wave reflected normal to the surface using the single parameter approach of *Chessell* [1977].

5. Detectability and Noise

5.1. Turbulence

Instabilities in the thermal and viscous boundary layers near the surface form eddies in the atmosphere. Further instabilities cause these eddies to break down into continually smaller eddies until the energy is dissipated by viscosity. This statistical distribution of eddies, called turbulence, is at all times present in the atmosphere. The intensity of the turbulence is strongly dependent on meteorological conditions and height above the surface [*Piercy et al.*, 1977].

The turbulence creates random fluctuations in the atmosphere's refractive index, which produce random fluctuations in the phase and amplitude of the passing wave. The resulting phase differences in the direct and refracted wave paths create interference patterns causing the amplitude to fluctuate.

Daigle et al. [1983] used a model based on a simplified theory of homogeneous and isotropic turbulence with a Gaussian distribution of eddy size, L. For the case where $(r\lambda)^{1/2} \ll L$, the square log-amplitude and phase fluctuations, $\langle \chi^2 \rangle = \langle (\ln A/A_o)^2 \rangle$ and $\langle S^2 \rangle = \langle (\phi - \phi_o)^2 \rangle$, respectively, are given by

$$\langle \chi^2 \rangle = \langle S^2 \rangle = (\sqrt{\pi}/2) \langle \mu^2 \rangle k^2 r L, \tag{18}$$

where A, ϕ and A_o, ϕ_o are respectively the amplitude and phase in the presence and absence of turbulence, k is the wave number, and μ is the fluctuation in the acoustical index of refraction which *Daigle et al.* [1983] calculated from the approximation

$$\langle \mu^2 \rangle = \sigma_v^2 / c_o^2 + \sigma_T^2 / 4T_o^2, \tag{19}$$

where σ_v^2 and σ_T^2 are the standard deviation of the wind velocity and temperature fluctuations, respectively, c_o is the mean speed of sound, and T_o is the mean temperature. They found $\langle \mu^2 \rangle$ experimentally in the terrestrial case to range from 1×10^{-6} on a calm day to 10×10^{-6} on more turbulent days.

This theory predicts that the phase and amplitude fluctuations increase with increasing distance of propagation, frequency, and strength of turbulence. For longer distances and/or stronger turbulence, a point is reached in which the phase fluctuations have a standard deviation comparable to 90°, and the signal becomes uncorrelated with the source. This phenomena, termed saturation, is the point where amplitude fluctuations are limited to a standard deviation. *Embleton et al.* [1974] and *Daigle et al.* [1983] found this to be no more than ~6 dB for terrestrial examples.

The effect of turbulence on Mars is uncertain. Modeling by *Savijärvi* [1991], *Sutton et al.* [1979], and *Tillman et al.* [1994] suggest turbulence is significantly greater on Mars than on Earth and varies with the diurnal fluctuations of solar insulation at the surface, peaking in the late Martian morning. The Mars Pathfinder Atmospheric Structure Investigation/Meteorology (ASI/MET) experiment pressure sensors detected pressure fluctuations of the magnitude 0.1-5 N m^{-2} on timescales ranging from seconds to hours. These appeared to be correlated with wind and temperature fluctuations and were largest in late morning and early afternoon when the boundary layer was most turbulent [*Schofield et al.*, 1997]. Since turbulence introduces random fluctuations in the pressure signal level received by a sensor with increasing distance from the source, identifying more distant sources becomes increasingly difficult as the signal to noise ratio will decrease with distance as a result.

In a truly static atmosphere, i.e., a continuous gaseous medium without any extraneous thermal or mechanical perturbations, there will be an intrinsic fluctuation in the pressure due to random molecular motions. The fluctuations in the number density of a gas are of the order $n^{-1/2}$ [*McQuarrie*, 1973], which for an ideal gas corresponds to pressure fluctuations of the order 10^{-33} N m^{-2} on Mars. The number of molecules striking a given surface per unit area ϕ_o, i.e., a sensor of some kind, will correspondingly fluctuate such that $\phi_o = p^* (2\pi mkT)^{-1/2}$, where p^* is the fluctuation in pressure and k is Boltzmann's constant [*Reif*, 1965]. It can be seen that a sensor's sensitivity to these fluctuations will be a function of the sensor's surface area. It turns out that these fluctuations are negligible compared to the 0 dB sound level, which corresponds to a pressure signal level of the order of 10^{-6} N m^{-2}, the approximate sensitivity level of the Mars microphone in the terrestrial environment (G. T. Delory et al., unpublished manuscript, 2000).

5.2. Atmospheric Profile

The daytime temperature profile of the Mars Pathfinder landing site was characterized by turbulent mixing revealed by rapid temperature fluctuations due to surface heating. The nighttime boundary layer, however, experienced a stably stratified condition [*Schofield et al.*, 1997] which is consistent with modeling done by *Haberle et al.* [1993], *Savijärvi* [1991], and *Gierasch and Goody* [1968]. This nighttime inversion will act to refract upward traveling acoustic rays back toward the surface creating a ducting effect with the planet's surface enabling sounds to travel greater distances. Since the turbulence is subdued during this period, the nighttime may offer the best atmospheric conditions for sampling the acoustic environment. During the primary mission, the Mars Polar Lander would not have experienced darkness as the sun would not have actually set. There would, however, be modulation of insolation since the landing site was ~14° south of the geometric pole and a diurnal variation in surface temperatures would result creating thermal inversions tens to hundreds of meters in thickness (M. Richardson, personal communication, 1999).

6. Acoustic Sources

It is useful to consider a few sound sources that a future acoustic sensor may detect at the Martian surface. The microphone is expected to detect the various sounds generated by the Mars Polar Lander itself due to their close proximity to the instrument. The robotic arm generates a characteristic dual frequency that has been recorded by the microphone in the lab under terrestrial conditions (G. T. Delory et al., unpublished manuscript, 2000). Other noises generated by the lander include the opening of the Thermal and Evolved Gas Analyzer (TEGA) doors for soil analysis as these are pyrotechnically initiated events as well as the motors on the camera.

Aside from the noises generated by the operation of the lander itself, the principle source of sound is likely to be aeroacoustic noises generated by wind as it flows past the

lander and its components. From the acoustic measurements taken by the Russian Groza-2 instrument aboard the Venera 13 and 14 landers at the surface of Venus, *Ksanfomaliti* [1982] found this to be the only identifiable source of sound not generated by the operation of the systems on board the spacecraft [see, also, *Ksanfomaliti*, 1983].

Aeroacoustic sound, the acoustic phenomena accompanying the flow of gas past a solid body, is largely determined by the Reynolds number [*Goldstein*, 1976]. At Reynolds numbers between 50 and 10^5, the periodic shedding of vortices takes place, exerting a periodic lift force on the solid body that can give rise to pure tones, referred to as aeolian tones. Aeolian tones were first investigated by *Strouhal* [1878] who determined the frequency of vortex shedding to be $f=S_tU/D$, where U is the wind speed, D is the characteristic diameter of the rigid solid, and S_t is the Strouhal number which depends on the Reynolds number but its value remains close to 0.2 [*Gerrard*, 1955; *Blevins*, 1984]. *Curle* [1955], utilizing the theory presented by *Lighthill* [1952] on the aerodynamic production of sound, demonstrated that the intensity of the sound generated is proportional to $\rho_o U^6 c^{-3} D^2 r^{-2}$, where c is the sound speed and r is the distance from the source.

The various components of a lander, including the main body itself, are potential sources of aeroacoustic sound. A general range of frequencies expected to be generated by the various lander components can be estimated. For wind speeds of 1-20 m s^{-1} [*Lorenz*, 1997], the robotic arm ($D \sim 5$ cm) and the meteorologic mast ($D \sim 2$ cm) of MPL, for example, would be expected to have produced frequencies in the range 4 – 80 Hz and 10 – 200 Hz, respectively. The relative magnitudes of the sounds will ultimately depend on the direction of the wind and the proximity of the source to the microphone.

Sand-sized particles may also be present in the Martian south polar layered deposits. Although thermal inertia data of the region suggest the area is mantled by dust size particles, imaging data reveals localized deposits of dark, dune material throughout the layered terrain [*Vasavada et al.*, 2000; *Herkenhoff and Murray*, 1990a, b]. Saltating materials blown against a microphone or lander may be detectable by an instrument.

The acoustic emissions of booming sand dunes has also been suggested to exist in the Martian environment [*Criswell et al.*, 1975; *Lindsay et al.*, 1976]. Studies have shown that booming of sand occurs in very dry climates with sand grains of smooth subdued surface textures, the lithology of which appears to not be important. Microphone recordings of booming dunes reveal acoustic emissions in narrow frequency bands, the peak value ranging from 50 to 100 Hz. Although a rare phenomena on Earth, *Lindsay et al.* [1976] suggests this may be common on Mars.

Large meteor - fireballs or bolides (bodies > 20 cm) offer another mechanism for creating sounds and are known to enter the terrestrial atmosphere quite frequently generating hypersonic booms, including multiple booms [*ReVelle*, 1997a]. Meteors that penetrate the atmosphere deep enough to obtain continuum flow conditions typically have entry speeds 35-100 times the local sound speed and can therefore be modeled as a line source of initially, nonlinear blast waves whose wavefronts are essentially perpendicular to the entry trajectory [*ReVelle*, 1976]. Nearly spherical wavefronts close to the end of trajectory can also be generated by a point source-type explosion during entry if terminal gross fragmentation occurs [*Ceplecha et al.* 1998]. The source energies of such meteor - fireballs range from 10^{-3} to 10^5 kt (kiloton equivalent of TNT where 1 kt = 4.185×10^{12} J) with nonlinear blast wave radii of a few meters to a few kilometers.

Far from the trajectory, the frequency of the associated acoustic wave will be proportional to the ratio of the local sound speed and the blast wave radius [*ReVelle*, 1976]. This gives a frequency range of ~0.1 – 120 Hz for an air temperature of 220 K and blast wave radii of a few meters to a few kilometers. For smaller meteors, the frequencies generated are high enough that classical and molecular absorption will dominate the removal of the acoustic signal before it can propagate very far. As the blast waves typically occur at altitudes > 30 km in the terrestrial environment, a detectable acoustic signal most likely will never reach the surface of Mars.

The acoustic signals generated at the very low frequencies in the infrasound, capable of propagating distances exceeding their source altitude, will be refracted away from the surface under conditions of normal atmospheric lapse rate. For a given lapse rate, there will be a critical ray that reaches the surface at grazing angles, beyond which only sound scattered by atmospheric inhomogeneities will reach the surface. The distance scale that this occurs is $D \approx 2(hT_o/\Gamma)^{1/2}$, where h is the altitude of the source, T_o is the average profile temperature, and Γ is the lapse rate [*Fleagle and Businger*, 1980]. For a temperature of 220 K, an altitude of 20 km, and a lapse rate of -4.5 K km^{-1} (the dry adiabatic value of the lower Martian atmosphere [*Zurek*, 1992]), the horizontal distance from which direct acoustic ray paths from an elevated point source will intersect the ground is ~62.5 km.

ReVelle et al. [1997b] has estimated that ~10,000-30,000 bolides penetrate the Earth's atmosphere globally each year. Approximating the influx of bolides into the Martian atmosphere to be roughly double that of Earth due to its closer proximity to the asteroid belt [*Wetherill*, 1989], the probability that a meteor - fireball will pass within a radius of 62.5 km in a 90 day period, the expected length of the Mars Polar Lander mission, is ~15 - 54 %.

One common acoustic source on Earth that is known to exist on Mars is dust devils. Dust devils have been identified in Viking images where they have been observed to ranged in size from 1 to 6 km in height and up to 1 km in diameter at their tops, the most typical dust devils being 2 km in height and 200 m in diameter [*Thomas and Gierasch*, 1985]. *Schofield et al.* [1997] interpreted pressure features with minima of 1-5 N m^{-2} and durations less than a minute to be dust devils passing over the Pathfinder landing site. More recently, *Metzger* [1999], using the Mars Orbital Camera of the Mars Global Surveyor spacecraft, noted further evidence of dust devils including tracks upon the Martian surface created by the passage of these vorticities. Infrasonic sound waves of terrestrial tornadoes and funnel clouds have been noted. *Cook and Young* [1962] observed the arrival of infrasound at Washington D.C. generated by several tornadic storms over Oklahoma and noted that they had prominent periods between 12 and 50 s (0.08-0.02 Hz) with amplitudes up to ~0.1 N m^{-2}. A detector sensitive to these low frequencies may detect Martian dust devils at large distances. Higher frequency sounds (up to 2000 Hz) have been recorded

within close proximity ($\lesssim$ 300 m) of tornadoes in the terrestrial environment [*Arnold et al.*, 1976]. If these large dust devils occur in the region of the MPL landing site, then there is good chance that the microphone could have detected it.

It has been theorized that electrostatic discharge in the Martian atmosphere is possible during strong surface winds with extremely large dust mass loading, i.e., large dust storms and dust devils. Modeling by *Melnik and Parrot* [1998] has shown that the electrical breakdown voltage can be attained in a Martian dust storm owing to the planet's lower atmospheric pressure. Experimental results of *Eden and Vonnegut* [1973] in 10 mbar CO_2 showed visible breakdown and measured potential gradients of 5 kV m^{-1} when dust was agitated. This may have been a potential acoustic source during the MPL mission as large dust storms are know to originate in the high southern latitudes during the late southern spring.

Propagating seismic waves can generate an acoustic wave train in cases where the phase velocity of the seismic wave is equal to the sound speed in air. *Kitov et al.* [1997] analyzed several near and below surface explosions and found seismically induced acoustic waves could be effectively propagated with dominant frequencies ~1-2 Hz. *Cook and Young* [1962] and were able to identify seismically induced infrasound of S wave and Rayleigh wave arrivals of an earthquake at a distance of 2860 km. A microphone sensitive to these low frequencies could detect seismic events [*ReVelle*, 1976].

The microphone aboard MPL was limited in its detectability as it was a very simple instrument. Its calibration had not been completed and its response to low frequencies and intensities remains unknown. Whether it would have been capable of detecting frequencies in the infrasonic range was under investigation. The minimum detectable intensity was also under investigation as it had been found that the microphone response for a 1 kHz sound dropped by ~25-28 dB between Earth and Mars pressures.

7. Comments

Several factors that will effect sound on Mars and its ability to propagate have not been addressed. One approximation that has been made is the assumption of a purely CO_2 atmosphere. Minor constituents are mixed within the CO_2 which include diatomic nitrogen (2 %) and argon-40 (1.6 %). These are expected to have a minor effect. *Shields* [1957] noted an influence on molecular relaxation of CO_2 due to impurities on experimental results. Also, the effect of water and CO2 ice crystals that can form clouds and ground fogs as well as dust storms that have the ability to suspend dust particles for extended periods of time in the atmosphere have been neglected. Dust and fog are known to cause attenuation and dispersion below a few hundred Hz in the terrestrial environment [*Henley and Hoidale,* 1973; *Davidson,* 1977]. Strong winds will also deflect sounds and curve the ray path of the propagation. Weather fronts are capable of effectively blocking the passage of sound.

Diffusion of sound around obstructions will also occur where wavelengths are small relative to objects. The shape of the propagating wave front will be distorted as portions of the wave front are removed by objects surrounding the microphone, creating sound shadows where the intensity will be diminished.

8. Conclusion

Sounds detectable by the human ear, frequencies in the range 20 – 20,000 Hz, will be more severely attenuated on Mars than the terrestrial environment. For example, a plane wave propagating on Mars, excluding environmental factors such as wind, turbulence, and the ground, will be attenuated at a rate of 0.419 and 8.98 dB m^{-1} at 20 Hz and 20 kHz respectively. On Earth, the attenuation rate will be $9x10^{-4}$ and 0.572 dBm^{-1} at 20 Hz and 20 kHz, respectively. Sounds in the infrasonic range will travel appreciably greater distances as the attenuation rate begins to resemble that of the terrestrial environment as classical and molecular absorption become less important. Sounds at the lower end of the audible spectrum (< 3000 Hz) can be expected to propagate tens of meters, but probably no more than 100 meters.

The Mars Microphone could be expected to have detected various sounds produced from processes generated by the Mars Polar Lander due to their close proximity. Aeroacoustic noise is also likely to have been present as well as the sound of sand grains blowing against the instrument. Electrical discharges in dust storms, large-scale dust devils, or explosive meteoritic events are other possible sources of sound that may exist in the Martian surface environment.

The most interesting sounds on Mars will probably be in the infrasonic frequency range, i.e., <20 Hz, as these frequencies are capable of traveling greater distances. Sound sources such as meteors penetrating the atmosphere, Mars-quakes, and meteorological phenomena can be expected to propagate large distances at very low frequencies.

The Surface Science Package (SSP) of the Huygens Titan probe on its way to the Saturn system as part of the Cassini mission, arriving in the year 2004, includes acoustic instruments to study the properties of the surface and atmosphere of the moon Titan [*Zarnecki*, 1992]. This will provide another opportunity to sample sounds from the surface of an extraterrestrial body in the future.

Acknowledgments. I would like to thank David A. Paige and William I. Newman of the University of California, Los Angeles, Department of Earth and Space Sciences for their guidance and financial support and invaluable input from Ian McEwan and Ashwin Vasavada of the MVACS team at UCLA and Nita Nee Lawson. I would also like to thank Ralph Lorenz and an anonymous reviewer for useful comments and suggestions that greatly improved the paper. This paper was supported by the MVACS missions operations for the Mars Polar Lander mission, grant number JPL 1203132.

References

Arnold, R. T., H. E. Bass, and L. N. Bolen, Acoustic spectral analysis of three tornadoes, *J. Acoust. Soc. Am.*, *60*, 584-593, 1976.

Attenborough, K., Acoustical characteristics of rigid fibrous absorbents and granular materials, *J. Acoust. Soc. Am.*, *73*, 785-799, 1983.

Blevins, R. D., Review of sound induced by vortex shedding from cylinders, *J. Sound Vibration*, *92*, 455-470, 1984.

Ceplecha, Z., J. Borovicka, W. G. Elford, D. O. ReVelle, R. L. Hawkes, V. Porubcan, and M. Simek, Meteor phenomena and bodies, *Space Sci. Rev.*, *84*, 327-471, 1998.

Chessell, C. I., Propagation of noise along a finite impedance boundary, *J. Acoust. Soc. Am.*, *62*, 825-834, 1977.

Cook, R. K., and J. M. Young, Strange sounds in the atmosphere: Part 2, *Sound*, *1*, 25-33, 1962.

Criswell, D. R., J. F. Lindsay, and D. L. Reasoner, Seismic and acoustic emissions of a booming dune, *J. Geophys. Res.*, *80*, 4963-4973, 1975.

Curle, N., The influence of solid boundaries upon aerodynamic sound, *Proc. R. Soc. London, Ser. A, 231*, 505-514, 1955.

Daigle, G. A., J. E. Piercy, and T. F. W. Embleton, Line-of-sight propagation through atmospheric turbulence near the ground, *J. Acoust. Soc. Am., 74*, 1505-1513, 1983.

Davidson, G. A., Propagation of audible sound through air-water fogs, *J. Acoust. Soc. Am., 62*, 497-502, 1977.

Delany, M. E., and E. N. Bazley, Acoustical properties of fibrous absorbent materials, *Appl. Acoust., 3*, 105-116, 1970.

Eden, H. F., and B. Vonnegut, Electrical breakdown caused by dust motion in low pressure atmospheres: Considerations for Mars, *Science, 180*, 962-963, 1973.

Embleton, T. F. W., Tutorial on sound propagation outdoors, *J. Acoust. Soc. Am., 100*, 31-48, 1996.

Embleton, T. F. W., N. Olson, J. E. Piercy, and D. Rollin, Fluctuations in the propagation of sound near the ground, *J. Acoust. Soc. Am., 55*, 485, 1974.

Embleton, T. F. W., J. E. Piercy, and G. A. Daigle, Effective flow resistivity of ground surfaces determined by acoustical measurements, *J. Acoust. Soc. Am., 74*, 1239-1244, 1983.

Fleagle, R. G., and J. A. Businger, *An Introduction to Atmospheric Physics*, 2nd ed., 367 pp., Academic, San Diego, Calif., 1980.

Gerrard, J. H., Measurements of the sound from circular cylinders in an air stream, *Proc. Phys. Soc. B, 68*, 453-461, 1955.

Gierasch, P., and R. Goody, A study of the thermal and dynamical structure of the Martian lower atmosphere, *Plant. Space Sci., 16*, 615-646, 1968.

Goldstein, M. G., *Aeroacoustics*, 1st ed., 293 pp., McGraw-Hill, Inc. New York, 1976.

Haberle, R. M., H. C. Houben, R. Hertenstein, and T. Herdtle, A boundary-layer model for Mars: Comparison with Viking lander and entry data, *J. Atmos. Sci., 50*, 1544-1559, 1993.

Henley, D. C., and G. B. Hoidale, Attenuation and dispersion of acoustic energy by atmospheric dust, *J. Acoust. Soc. Am., 54*, 437-444, 1973.

Herkenhoff, H.E., and B.C. Murray, Color and albedo of the south polar layered deposits on Mars, *J. Geophys. Res., 95*, 1343-1358, 1990a.

Herkenhoff, H.E., and B. C. Murray, High-resolution topography and albedo of the south polar layered deposits on Mars, *J. Geophys. Res., 95*, 14511-14529, 1990b.

Keenan, J. H., J. Chao, and J. Kaye, *Gas Tables,* 2nd ed., 211 pp., John Wiley, New York, 1983.

Kinsler, L. E., R. F. Austin, A. B. Coppens, and J. V. Sanders, *Fundamentals of Acoustics*, 3rd ed., 480 pp., John Wiley, New York, 1982.

Kitov, I. O., J. R. Murphy, O. P. Kusnetsov, B. W. Barker, and N. I. Nedoshivin, An analysis of seismic and acoustic signals measured from a series of atmospheric and near-surface explosions, *Bull. Seismol. Soc. Am., 87*, 1553-1562, 1997.

Ksanfomaliti, L. V., N. V. Goroshkova, and M. K. Naraeva, Acoustic measurements of the wind velocity at the Venera-13 and Venera-14 landing sites, *Sov. Astron. Lett. Engl. Trans., 8*, 227-229, 1982.

Ksanfomaliti, L. V., N. V. Goroshkova, and V. K. Khondyrev, Wind velocity near the surface of Venus from acoustic measurements, *Cosmic Res. Engl. Trans., 21*, 161-167, 1983.

Lighthill, M. J., On sound generated aerodynamically, I., General theory, *Proc. R. Soc. London, Ser. A, 211*, 564-587, 1952.

Lindsay, J. F., D. R. Criswell, T. L. Criswell, and B. S. Criswell, Sound-producing dune and beach sands, *Geol. Soc. Am. Bull., 87*, 463-473, 1976.

Lorenz, R. D., Martian surface wind speeds described by the Weibull distribution, *J. Spacecr. Rockets, 33*, 754-756, 1997.

Marion, J.B., and S. T. Thornton, *Classical Dynamics of Particles and Systems*, 4th ed., 638 pp., Saunders College Publishing, Fort Worth, Tex., 1995.

Mase, G.E., *Schaum's Outline of Theory and Problems of Continuum Mechanics*, 1st ed., 221 pp., McGraw-Hill, New York, 1970.

McQuarrie, D. A., *Statistical thermodynamics,* 1st ed., 343 pp., Harper Collins, New York, 1973.

Melnik, O., and M. Parrot, Electrostatic discharge in Martian dust storms, *J. Geophys. Res., 103*, 29,107, 1998.

Metzger, S. M., Feeding the Mars dust cycle: surface dust storage and dust devil entrapment, paper, presented at The Fifth International Conference on Mars, Lunar and Planetary Institute, Pasadena, California, July 18-23, 1999.

Morse, P.M., and K. U. Ingard, *Theoretical Acoustics*, 1st ed., 927 pp., McGraw-Hill, New York, 1968.

Piercy, J. E., Role of the vibrational relaxation of nitrogen in the absorption of sound in air, *J. Acoust. Soc. Am., 46*, 602-604, 1969.

Piercy, J. E., T. F. W. Embleton, and L. C. Sutherland, Review of noise propagation in the atmosphere, *J. Acoust. Soc. Am., 61*, 1403-1418, 1977.

Reif, F., *Fundamentals of Statistical and Thermal Physics*, 1st ed., 651 pp., McGraw-Hill, New York, 1965.

ReVelle, D. O., On meteor-generated infrasound, *J. Geophys. Res., 81*, 1217-1230, 1976.

ReVelle, D. O., Historical detection of atmospheric impacts by large bolides using acoustic-gravity waves, *Proc. S.P.I.E. Int. Soc. Opt. Eng., 822*, 284-302, 1997.

ReVelle, D. O., R. W. Whitaker, and W. T. Armstrong, Infrasonic observations of bolides on October 4, 1996, *Proc. S.P.I.E., 3116*, 156-167, 1997.

Savijärvi, H., A model study of the PBL structure on Mars and the Earth, *Beitr. Phys. Atmos., 64*, 219-229, 1991.

Schofield, J. T., J. R. Barnes, D. Crisp, R. M. Haberle, S. Larson, J. A. Magalhaes, J. R. Murphy, J. R. Seiff, and G. Wilson, The Mars Pathfinder atmospheric structure investigation/meteorology (ASI/MET) experiment, *Science, 278*, 1752-1758, 1997.

Shields, F.D., Thermal relaxation in carbon dioxide as a function of temperature, *J. Acoust. Soc. Am., 29*, 450-454, 1957.

Strouhal, V., Ueber eine besondere art der tonenegung, *Ann. Phys. Leipzig, 5*, 216-251, 1878.

Sutton, J. L., C. B. Leovy, and J. E. Tillman, Diurnal variations of the Martian surface layer meteorological parameters during the first 45 sols at two Viking lander sites, *J. Atmos. Sci., 35*, 2346-2355,1978.

Thomas, P., and P. J. Gierasch, Dust devils on Mars, *Science, 230*, 175-177, 1985.

Tillman, J. E., L. Landberg, and S. E. Larsen, The boundary layer of Mars: Fluxes, stability, turbulent spectra, and growth of the mixed layer, *J. Atmos. Sci., 51*, 1709-1727, 1994.

Touloukian, Y. S., P. E. Liley, and S. C. Saxena, *Thermal Conductivity, Nonmetallic Liquids and Gases*, 1st ed., 531 pp., Plenum, New York, 1970.

Touloukian, Y. S., S. C. Saxena, and P. Hestermans, *Viscosity*, 1st ed., 643 pp., Plenum, New York, 1975.

Vasavada, A. R., J. P. Williams, D. A. Paige, R. Greeley, B. C. Murray, K. E. Herkenhoff, N. T. Bridges, D. S. Bass, and K. S. McBride, Surface properties of Mars' polar layered deposits and polar lander sites, *J. Geophy. Res., 105*, 6961-6969, 2000.

Wetherill, G. W., Cratering of the terrestrial planets by apollo objects, *Meteoritics, 24*, 15-22, 1989.

Zarnecki, J. C., Surface science package for the Huygens Titan probe, *J. Br. Interplanet. Soc., 45*, 365-370, 1992.

Zurek, R.W., Comparative aspects of the climate of Mars: an introduction to the current atmosphere, in *Mars*, edited by H. H. Kieffer, et al., pp. 799-817, Univ. of Ariz. Press, Tucson, 1992.

J.-P. Williams, Department of Earth and Space Sciences, University of California, Los Angeles, CA 90095. (jpierre@mvacs.ess.ucla.edu)

(Received September 7, 1999; revised November 26, 1999; accepted December 7, 1999.)